# Optimal Mixing on the Sphere

Amanda K. O'Rourke

November 10, 2010

## 1 Introduction

The mixing of tracers on the surface of a sphere has many geophysical applications from the advection of volcanic ash to the global redistribution of temperature and angular momentum by atmospheric general circulation. Due to the difficulties of spherical geometry, such as the poles and the isotropy between the meridional and zonal directions, previous work on optimal mixing focuses instead on the $d$-dimensional torus [5, 7, 8]. Here we are motivated by the geophysical problem of temperature redistribution over the surface of the sphere given a heat source at the equator and cooling at the poles. What flow most efficiently mixes the temperature field and how do the characteristics of these optimal flows compare to similar flows on the torus?

Before describing the properties of optimal flows, we must first define a measure of mixing efficiency that will then be used to define a flow that most optimally mixes a tracer field. One measure of mixing is the variance of the tracer concentration. If we consider the time evolution of a tracer field with zero mean subject to advective stirring and diffusivity, the tracer concentration $\theta$ obeys the advection-diffusion equation

$$\frac{\partial \theta}{\partial t} + \boldsymbol{u} \cdot \nabla \theta - \kappa \Delta \theta = 0 \tag{1}$$

where $\boldsymbol{u}$ is the advective velocity (independent of the tracer concentration $\theta$) and where $\kappa$ is the molecular diffusivity coefficient. Multiplying (1) by $\theta$ and averaging over the domain yields the time rate of change of the variance of $\theta$ given by

$$\frac{\partial \langle |\theta|^2 \rangle}{\partial t} = -2\kappa \langle |\nabla \theta|^2 \rangle \tag{2}$$

where the integral over the domain $V$ is denoted by

$$\langle \theta \rangle = \frac{1}{V} \int_V \theta dV. \tag{3}$$

From (3) we see that the variance of the tracer concentration $\langle |\theta|^2 \rangle$ decreases monotonically as a function of the molecular diffusivity $\kappa$ and the magnitude of the gradients of the tracer field. As both $\kappa$ and $\langle |\nabla \theta|^2 \rangle$ are positive definite, the variance of the tracer tends to a constant as the gradients of the tracer field tend to zero in the absence of sources or sinks of the tracer. In other words, diffusion acts to destroy gradients in the tracer field and homogenize $\theta$.

Diffusivity can reduce the variance of a tracer field in the absence of stirring, however this process of diffusive mixing is quite inefficient. We can significantly enhance the process of mixing and homogenization by including a stirring flow $\boldsymbol{u}$. The mechanical act of stirring stretches and folds material lines of the tracer field, enhances the gradients of $\theta$, and ultimately leads to a more rapid homogenization of the tracer field.

If there are no source terms to maintain gradients in $\theta$ diffusivity will lead to a spatially homogeneous tracer field over time. We can obtain a nonzero $\langle|\theta|^2\rangle$ as $t \to \infty$ by including a spatially varying tracer source term in (1),

$$\frac{\partial \theta}{\partial t} + \boldsymbol{u} \cdot \nabla \theta - \kappa \Delta \theta = s(\boldsymbol{x}). \tag{4}$$

The homogenization of the tracer field by mixing can then balance the production of tracer variance by the source in steady state. It is within this steady state that we will evaluate the effect of stirring on the mixing process.

As we expect stirring to enhance mixing, we anticipate that for the same value of $\kappa$ the variance of a stirred tracer field will be less than that of an unstirred tracer in steady state. Thiffeault et al. [7] measure the relative mixing enhancement due to stirring through a measure given by ratio of the unstirred to stirred steady state variances,

$$\mathcal{E}^2 = \frac{\langle|\theta_0|^2\rangle}{\langle|\theta|^2\rangle}. \tag{5}$$

where $\theta_0$ satisfies the unstirred, steady state diffusion equation

$$-\kappa \Delta \theta_0 = s(\boldsymbol{x}) \tag{6}$$

and where $\theta$ satisfies the stirred, steady state advection-diffusion equation

$$\boldsymbol{u} \cdot \boldsymbol{\nabla} \theta - \kappa \Delta \theta = s(\boldsymbol{x}). \tag{7}$$

A mixing efficiency of $\mathcal{E} = 1$ would imply that the velocity field does not enhance mixing relative to diffusive processes, as would be the case if $\boldsymbol{u}$ were parallel to lines of constant $\theta$ such that the advective term $\boldsymbol{u} \cdot \nabla \theta$ of (4) vanished. Mixing efficiencies of $\mathcal{E} < 1$ will be obtained if $\boldsymbol{u}$ enhances gradients of $\theta$ in steady state. Such small mixing efficiencies are counterintuitive if we assume that stirring tends to *improve* the homogenization of a tracer with time, as is the case for flows with mixing efficiencies of $\mathcal{E} > 1$.

By defining the mixing efficiency factor $\mathcal{E}$ we can then create an optimization problem to determine the most efficient flow fields over the surface of the sphere by maximizing $\mathcal{E}$. Many approaches have been taken to this problem in the past, however all have focused on flows over the torus. There are two primary methods of maximizing $\mathcal{E}$: finding the flow that most efficiently mixes a tracer field for a given source function or, alternatively, finding the source function that is most efficiently mixed by a fixed velocity field. Thiffeault and Pavliotis [8] consider the problem of optimizing the source function for a fixed velocity field and find that these sources tend to have maxima and minima located near in regions of strongest velocity and are aligned such that the flows transport sources over sinks.

Alternatively, Lin et al. [3] and Thiffeault [6] maximize the mixing efficiency for a fixed source by varying the velocity field. Lin et al. [3] determine the velocity field that most

quickly reduces a measure of mixing similar to $\mathcal{E}$ in the absence of diffusivity. In contrast to the transient problem considered by Lin et al. [3], Thiffeault [6] introduce a means of solving for the velocity fields that most efficiently mix a tracer concentration maintained by a spatially varying source term and subject to molecular diffusivity.

Both Lin et al. [3] and Thiffeault [6] find optimal velocity fields on the torus. Here we will expand on the approach of Thiffeault [6] to consider optimal flows over the surface of the sphere. We choose to focus on three points of comparisons between optimal flows on the torus and the sphere: the issue of upper and lower bounds on the mixing efficiencies, the structure of the most optimal flow configurations, and the scaling of the efficiencies in the Péclet number.

In Section 2 we describe the numerical model we will use to find velocity fields that maximize $\mathcal{E}$. We then compare the analytical lower bound of the mixing efficiencies on the torus to that of the sphere in Section 3 and see if the efficiencies scale as a function of the Péclet number on the sphere as they do on the torus in Section 4. We will then discuss the possibility of an efficient 'sweeping' flow for the sphere in Section 5. In Section 6 we consider future directions of this work.

# 2 The Model

## 2.1 Euler-Lagrange Equations

We maximize $\mathcal{E}$ in a spherical geometry by varying the advective velocity field while holding constant the structure of the source function and the diffusivity. The mixing efficiency $\mathcal{E}$ as given in (5) has two components: the variance of the unstirred steady state tracer field $\langle|\theta_0|^2\rangle$ and the variance of the stirred steady state tracer field $\langle|\theta|^2\rangle$. These tracer fields can be written as

$$\theta = \mathcal{L}^{-1}s \qquad\qquad \theta_0 = \mathcal{L}_0^{-1}s \tag{8}$$

where $\mathcal{L}$ and $\mathcal{L}_0$ are the advection-diffusion and diffusion operators given by

$$\mathcal{L} = \boldsymbol{u}\cdot\boldsymbol{\nabla} - \kappa\Delta \qquad\qquad \mathcal{L}_0 = -\kappa\Delta. \tag{9}$$

From (8) and (9), we see that the solution $\theta_0$ to the diffusion-only differential equation will be constant under a change in $\boldsymbol{u}$. Changing $\boldsymbol{u}$ will only influence the steady state stirred tracer field $\theta$ such that maximizing $\mathcal{E}$ is equivalent to minimizing $\langle|\theta|^2\rangle$. In order to minimize $\langle|\theta|^2\rangle$ with respect to $\boldsymbol{u}$, we first define the variation of $\langle|\theta|^2\rangle$ following Thiffeault [6]

$$\delta\langle|\theta|^2\rangle = \delta\langle|\mathcal{L}^{-1}s|^2\rangle \tag{10}$$

where we have used $\theta = \mathcal{L}^{-1}s$ from (8).

As we are holding the source function constant, only the integral operator $\mathcal{L}^{-1}$ changes under a change in $\boldsymbol{u}$ such that

$$\delta\langle|\theta|^2\rangle = 2\langle\mathcal{L}^{-1}s\delta\mathcal{L}^{-1}s\rangle \tag{11}$$

which can be simplified using the identity $\delta\mathcal{L}^{-1} = -\mathcal{L}^{-1}\delta\mathcal{L}\mathcal{L}^{-1}$,

$$\delta\langle|\theta|^2\rangle = -2\langle\mathcal{L}^{-1}s\mathcal{L}^{-1}\delta\mathcal{L}\mathcal{L}^{-1}s\rangle. \tag{12}$$

After integrating (12) by parts, $\delta\langle|\theta|^2\rangle$ can be written in terms of the self-adjoint operator

$$\mathcal{A} = \mathcal{L}\mathcal{L}^{\dagger}, \tag{13}$$

where $\mathcal{L}^{\dagger} = -\boldsymbol{u}\cdot\boldsymbol{\nabla} - \kappa\delta$ is the adjoint of the advection-diffusion operator, such that

$$\delta\langle|\theta|^2\rangle = -2\langle\mathcal{A}^{-1}s\delta\mathcal{L}\mathcal{L}^{-1}s\rangle. \tag{14}$$

As the variation in the advection diffusion operator only depends on the variation of the velocity field, $\delta\mathcal{L} = \delta\boldsymbol{u}\cdot\boldsymbol{\nabla}$, we can write the variation of $\langle|\theta|^2\rangle$ in terms of $\delta\boldsymbol{u}$,

$$\delta\langle|\theta|^2\rangle = -2\langle\mathcal{A}^{-1}s\delta\boldsymbol{u}\cdot\boldsymbol{\nabla}\mathcal{L}^{-1}s\rangle. \tag{15}$$

The functional derivative of $\langle|\theta|^2\rangle$ with respect to $\boldsymbol{u}$ then is

$$\frac{\delta\langle|\theta|^2\rangle}{\delta\boldsymbol{u}} = -2\mathcal{A}^{-1}s\nabla\mathcal{L}^{-1}s. \tag{16}$$

We could find the extrema of $\langle|\theta|^2\rangle$ by finding the zeroes of (16), however this would tell us little about the structure of the most efficient flows without additional constraints. We place a constraint on the energy and restrict our attention to non-divergent flows by creating an extended functional of $\langle|\theta|^2\rangle$

$$\mathcal{F}(\boldsymbol{u}) = \langle|\theta|^2\rangle + \gamma\left(\langle|\boldsymbol{u}|^2\rangle - U^2\right) + \langle\nu\boldsymbol{\nabla}\cdot\boldsymbol{u}\rangle \tag{17}$$

whose variation with respect to $\boldsymbol{u}$ is

$$\frac{\delta\mathcal{F}[\boldsymbol{u}]}{\delta\boldsymbol{u}} = -\mathcal{A}^{-1}s\nabla\mathcal{L}^{-1}s + \gamma\boldsymbol{u} - \nabla\nu = 0. \tag{18}$$

Equation (18) is the Euler-Lagrange equation for the constrained optimization problem where $\gamma$ and $\nu$ are the Lagrange multipliers for the energy and non-divergence constraints, respectively. Flows that satisfy these constraints have a kinetic energy $\langle|\boldsymbol{u}|^2\rangle$ equal to a constant value $U^2$ and are non-divergent such that $\boldsymbol{\nabla}\cdot\boldsymbol{u} = 0$.

## 2.2 Numerical Model

There are numerous methods of finding velocity fields that maximize $\mathcal{E}$ and minimize $\langle|\theta|^2\rangle$. Thiffeault [6], for example, suggests a method to directly solve the Euler-Lagrange equations given in (18) for the velocity field. Here we consider an alternate means of finding the minima of $\langle|\theta|^2\rangle$. We perform a two-part optimization process based on Matlab's built-in nonlinear optimization routine `fmincon`. This routine, a part of Matlab's Optimization Toolbox, minimizes $\langle|\theta|^2\rangle$ subject to the non-divergence and energy constraints.

The `fmincon` routine minimizes $\langle|\theta|^2\rangle$ using the iterative interior point algorithm. At each iteration of $\boldsymbol{u}$ and $\mathcal{L}[\boldsymbol{u}]$, we must solve the advection-diffusion equation (8) for $\theta$. For

the torus problem, we can solve (8) for $\theta$ by generating an invertible, spectral advection-diffusion operator matrix $\mathcal{L}[\boldsymbol{u}]$. The tracer concentration $\theta$ is then obtained by solving the system of linear equations using this non-singular operator. Due to time limits, we were unable to generate a non-singular, spectral advection-diffusion operator for the sphere. In order to find optimal solutions, we instead solve (8) for $\theta$ using `fsolve` where `fsolve` is a built-in Matlab routine that solves a system of nonlinear equations. Resorting to `fsolve` leads to an increased computational cost in the spherical problem relative to the torus problem.

In addition to solving for $\theta$ using `fsolve` for varying $\boldsymbol{u}$, we must consider that not all variations in $\boldsymbol{u}$ are permitted due to constraints. The optimization problem is constrained in two ways: the kinetic energy of the flow is held fixed at a constant value and the flow field must be non-divergent. The energy constraint limits the complexity and strength of the flow such that the optimal flow field $\boldsymbol{u}$ in steady state satisfies

$$\langle |\boldsymbol{u}|^2 \rangle = U^2 \tag{19}$$

where $U$ is a constant equal to unity for all optimal and sub-optimal flows considered here.

The energy constraint (19), along with the coefficient of diffusivity $\kappa$ and the radius of the sphere $a$, allow us to calculate the Péclet number for a given flow,

$$Pe = \frac{Ua}{\kappa} \tag{20}$$

where $Pe$ is a nondimensional parameter relating the relative magnitude of the advective stirring to the molecular diffusivity in the advection-diffusion equation (1) such that mixing processes with large $Pe$ are advection-dominated. The radius of the sphere is held fixed at $a = 1$ so that the Péclet number of all experiments here is a function of the diffusivity only.

The non-divergence constraint $\boldsymbol{\nabla} \cdot \boldsymbol{u}$ can be satisfied by defining a streamfunction $\psi$ such that the zonal and meridional velocities over the sphere, $u$ and $v$ respectively, satisfy

$$u = -\frac{1}{a}\frac{\partial \psi}{\partial \phi} \qquad\qquad v = \frac{1}{a\cos\phi}\frac{\partial \psi}{\partial \lambda} \tag{21}$$

where $-\pi \leq \phi \leq \pi$ is the latitude and $0 \leq \lambda \leq 2\pi$ is the longitude. It should be mentioned that we are using a geophysical coordinate system where $\phi = 0$ is at the equator rather than standard spherical coordinates where the polar angle is typically zero at the north pole.

As we are interested in flows over the surface of a thin spherical shell, it is useful to recast all operators and variables in terms of spherical coordinates. We use a pseudo-spectral approach to calculating the advection-diffusion operator $\mathcal{L}$. Transformations between grid space and spherical harmonics in addition to the calculation of derivatives in spherical coordinates are performed using Algorithm 888, a package of Matlab routines for spherical harmonic functions [1]. Using Algorithm 888, we cast all scalars in terms of their spherical harmonics,

$$\theta(\lambda, \phi) = \sum_{n=0}^{\infty} \sum_{m=-n}^{n} \tilde{\theta}_n^m Y_n^m(\lambda, \mu) \tag{22}$$

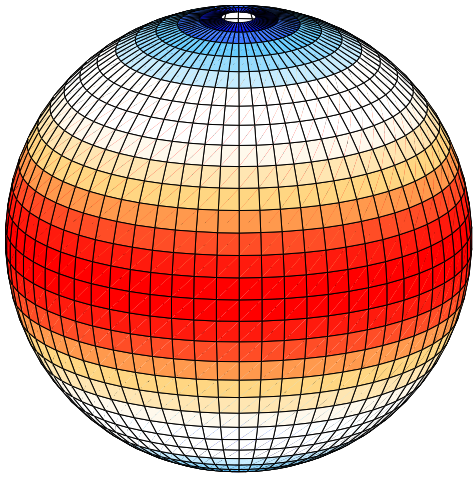

Figure 1: The geophysical source in arbitrary units, with heating (red) at the equator and cooling (blue) at the poles.

where $\tilde{\theta}$ is the spectral coefficient of $\theta$, $n$ is the total wavenumber, $m$ is the zonal wavenumber, and $Y_n^m(\lambda, \mu)$ is the spherical harmonic of longitude $\lambda$ and of $\mu = \sin\phi$. The spherical harmonic is given by

$$Y_n^m(\lambda, \mu) = e^{im\lambda} P_n^m(\mu). \tag{23}$$

where $P_n^m(\mu)$ are the associated Legendre functions defined by

$$P_n^m(\mu) = \frac{1}{2^n n!} \sqrt{\frac{(2n+1)\,(n-m)!}{2\,(n+m)!}} \left(1-\mu^2\right)^{m/2} \frac{d^{n+m}}{d\mu^{n+m}} \left(\mu^2-1\right)^n. \tag{24}$$

The wavenumbers $n$ and $m$ describe the structure of the scalar field in latitude and longitude. In the zonal direction, $m$ is similar to the $x$-wavenumber on the torus and is simply a superposition of Fourier modes. The geometries of the torus and the sphere, however, differ significantly in the meridional direction. Instead of a $y-$wavenumber as on the torus, spherical harmonics are cast in terms of a total wavenumber $n$ where $n-m$ are the number of nodes in the meridional direction.

The geophysical source function we consider here is given by the $n = 2$, $m = 0$ spherical harmonic with a spectral amplitude of $-1$. The source function can then be written as

$$s(\lambda, \phi) = (-1) Y_2^0(\lambda, \mu) = -P_2^0(\mu). \tag{25}$$

As $n - m = 2$ and $m = 0$ for the source function, $s(\lambda, \phi)$ has two nodes in latitude located in the midlatitudes and has no zonal structure. The amplitude is chosen so that there is a source of 'heat' at the equator and a sink at the poles, as shown in Figure 1.

### 2.3 Efficiencies of Sub-Optimal Flows

The `fmincon` routine is an iterative process that requires an initial velocity field sufficiently close to the optimal solution in order to converge on a minima in $\langle|\theta|^2\rangle$ with respect to $\boldsymbol{u}$. `Fmincon` can only identify local minima and, at this time, we are unable to state whether or not these optimal solutions minimize $\langle|\theta|^2\rangle$ globally. The solution space is littered with local minima such that a 'good' choice of an initial velocity field is crucial for both convergence and for the best chance at finding a true optimal velocity field $\boldsymbol{u}$.

In order to determine what constitutes a 'good' initial guess, we begin our investigation of optimal flows by determining the efficiencies of the sub-optimal flows generated by monochromatic streamfunctions. Thiffeault [6] note that the velocity fields that most efficiently mix a tracer in the presence tends to be flows that directly transport the tracer from regions of excess $\theta$ ('hot' regions, if we imagine the tracer is temperature) to sink ('cold') regions.

For the geophysical source in Figure 1 and following the observations of optimized source functions in Thiffeault and Pavliotis [8], the most optimal flow would likely be cellular with the strongest velocities over the maxima or minima of the source and nodes located near the mean value of $s(\boldsymbol{x})$. The geophysical source function achieves its mean value in the midlatitudes such that we would expect

$$\boldsymbol{u} = \left( -\frac{1}{a}\frac{\partial \psi}{\partial \phi}, \frac{1}{a\cos\phi}\frac{\partial \psi}{\partial \lambda} \right) \approx 0 \tag{26}$$

in these regions. Using (21), the streamfunction $\psi$ of this efficient flow would then likely achieve its extrema in the midlatitudes and have an inflection point near the equator. In terms of spherical harmonics, a streamfunction with wavenumbers satisfying $n - m = 1$, such as the monochromatic spherical harmonic functions $Y_2^1$ and $Y_3^2$, are good choices for $\psi$.

Indeed, $\psi \propto Y_3^2$ is the most efficient sub-optimal streamfunction at $Pe = 10$ over the range of monochormatic streamfunctions shown in Figure 2. Streamfunctions proportional to spherical harmonic modes $Y_n^m$ with $n-m = 1$ tend to have the highest mixing efficiencies, as expected, while those streamfunctions with $n - m = 0$ (inter-hemispheric flows) are slightly less efficient. In both the $n - m = 1$ and $n - m = 0$ flows, stirring enhances mixing such that $\mathcal{E} > 1$. Velocity fields described by streamfunctions with less zonal structure, or with smaller $m$, tend to be more efficient than those with larger values of $m$, with an optima in $\mathcal{E}$ around $m = 2$ for both $n - m = 1$ and $n - m = 0$. Good initial conditions for $\psi$ in the optimization algorithm would then be the monochromatic streamfunctions proportional to $Y_3^2$ and $Y_2^1$.

One surprising conclusion from Figure 2 is that some flows with $n - m = 2$ are in fact *inefficient*. For these flow fields, stirring actually increases $\langle|\theta|^2\rangle$ relative to the unstirred solution $\langle|\theta_0|^2\rangle$ resulting in $\mathcal{E} < 1$. It is clear that such flow fields would not be good initial guesses for the optimization problem as stirring acts to increase the variance of the steady

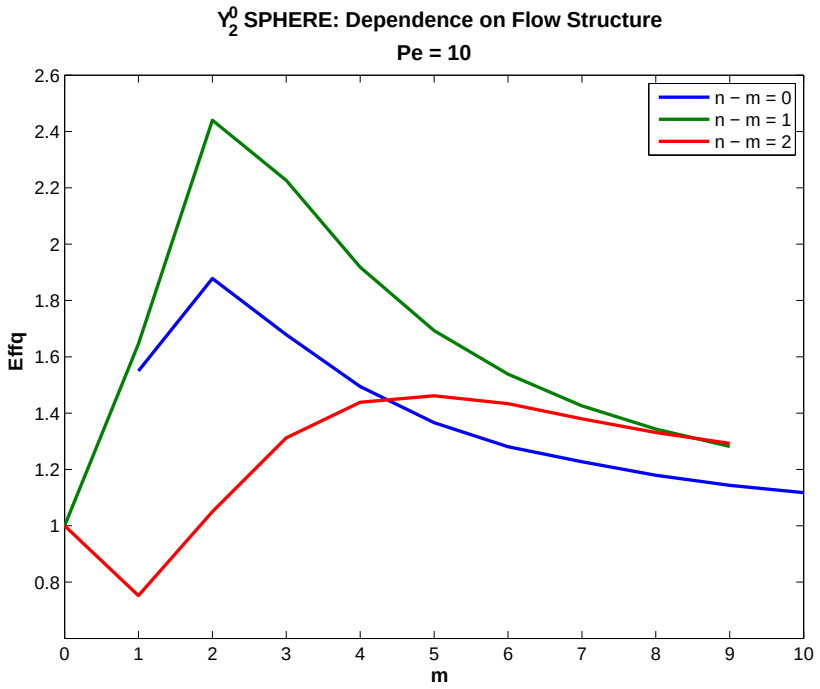


Figure 2: Sub-optimal efficiencies $\mathcal{E}$ for streamfunctions of the form $\psi \propto Y_n^m(\lambda, \mu)$ stirring the geophysical source field with $n - m = 0$ (blue), $n - m = 1$ (green), and $n - m = 2$ (red) for zonal wavenumbers $m = 0$ to 10 at $Pe = 10$.

state tracer field. These inefficient flows are a unique feature of spherical geometry and of our choice of steady, time-independent velocity fields as will be shown in Section 3.

# 3 Lower Bounds and Inefficient Stirring

In Section 2.3 we determined that not all stirring by a velocity field $\boldsymbol{u}$ enhances diffusive mixing. We obtained a range of sub-optimal efficiencies spanning both both positive and negative values of $\mathcal{E}$. What is the range of possible $\mathcal{E}$ for the sphere and how does this compare to that of the torus? We will answer this in two parts, focusing on the lower bounds and the existence of inefficient flows here and on the scaling of the most efficient flows in Section 4.

Previous work by Shaw et al. [5] obtained analytic upper and lower bounds on $\mathcal{E}$ for the torus by optimizing over the tracer field $\theta$. For tracer fields stirred by a uniform velocity field, where $\nabla \boldsymbol{u}(\boldsymbol{x}, t) = 0$ at each instant in time, and supplied by a monochromatic source, Shaw et al. [5] find that the mixing efficiencies are bounded by

$$1 \leq \mathcal{E}^2 \leq 1 + Pe^2/dL^2k_s^2 \tag{27}$$

where $d$ is the dimension of the torus, $L$ is the domain size, and $k_s$ is the wavenumber of the source. The Péclet number for the torus is the same as that of the sphere given in (20) with the domain size $L$ being the characteristic length in the place of the radius $a$.

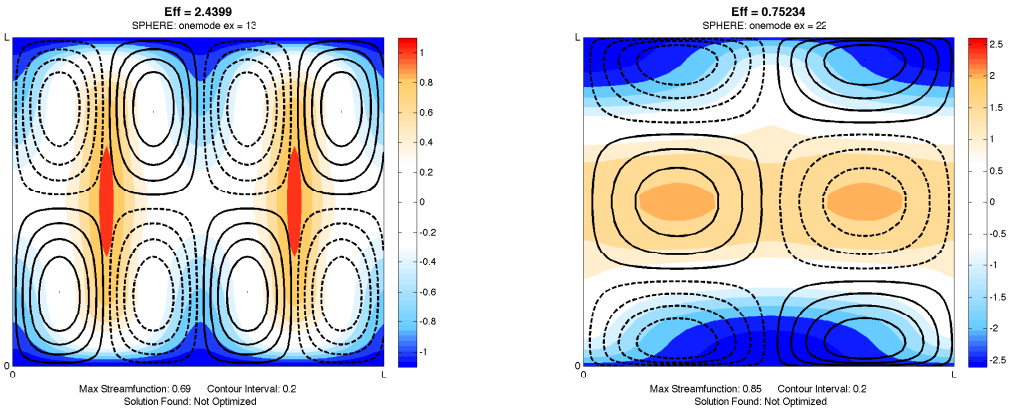


(a) Efficient Flow, $\mathcal{E} = 2.44$ (b) Inefficient Flow, $\mathcal{E} = 0.75$

Figure 3: Two of the sub-optimal flows associated with the parameter sweep in Figure 2 where Panel 3(a) is associated with the relatively efficient flow of mode $m = 2$, $n = 3$ and where Panel 3(b) is the inefficient flow of mode $m = 1$, $n = 3$. The streamfunction of the velocity field are plotted on top of colored contours of the steady-state tracer field $\theta$.

Shaw et al. [5] found that inefficient flows do not exist on the torus for monochromatic sources, such as the geophysical source function $s(\boldsymbol{x}) \propto Y_2^0(\lambda, \mu)$ that we consider here. For such monochromatic sources, stirring over the torus always acts to decrease the $\langle|\theta|^2\rangle$ in steady state relative to the unstirred solution. As we have already seen from Figure 2, inefficient flow not only exist for the geophysical source on the sphere–they are, in fact, fairly common. What are the properties of these inefficient flows that lead to an increase in the variance of $\theta$ relative to the unstirred solution?

If we compare the most efficient sub-optimal flow of Figure 2 to the most inefficient flow, we find that the concentration of the tracer field in steady state between Panel 3(a) and Panel 3(b) are quite different. The efficient flow has stagnation points centered near the mean value of the source function (located in the midlatitudes for the geophysical source) and strong zonal velocities near the source maxima and minima. In steady state, the warm patches of tracer are advected off equator in thin jets while cold regions are advected equatorwards, leading to efficient mixing of the tracer field relative to the diffusive-only solution.

The inefficient flow in Panel 3(b) has stagnation points centered on the equator at the region of maximum tracer input and strong flows parallel to lines of constant $\theta$. The maximum 'heating' at the equator is trapped at the stagnation points of the flow while the meridional flow everywhere is relatively weak. Without the ability to remove excess tracer at the equator and transport it to the sink at the poles, this flow tends to increase the tracer variance in steady state relative to the diffusive-only solution and thus has a mixing efficiency of $\mathcal{E} < 1$.

As for inefficient flows on the torus, Shaw et al. [5] identify that $\mathcal{E}$ satisfies

$$\mathcal{E}^2 = \frac{\langle|\theta_0|^2\rangle}{\langle|\theta|^2\rangle} \geq \frac{4\pi^2}{L^2}\frac{\langle|\Delta^{-1}s|^2\rangle}{\langle|\nabla^{-1}s|^2\rangle} = \frac{\sum_k (Lk/2\pi)^{-4}\,|\tilde{s}_{\boldsymbol{k}}|^2}{\sum_k (Lk/2\pi)^{-2}\,|\tilde{s}_{\boldsymbol{k}}|^2} \tag{28}$$

which they then solve using a variational problem in $\theta$ to maximize the stirred, steady state $\langle|\theta|^2\rangle$ subject to the steady state constraint $\kappa\langle|\nabla\theta|^2\rangle = \langle s\theta\rangle$.

The results of Shaw et al. [5] for a monochromatic source are due in part to the similarity between the the gradient and Laplacian operators in Fourier space, evident in the similarity in the numerator and denominator of the last term in (28). For a monochromatic source of wavenumber $k_s$, the Laplacian and gradient operators are simply

$$\nabla = ik_s \qquad\qquad \Delta = -k_s^2 \tag{29}$$

so that the Laplacian operator is the square of the gradient operator.

In terms of spherical harmonics, however, the gradient operator is significantly different from the Laplacian. The Laplacian of the spherical harmonic function $Y_n^m$ is given by

$$\Delta Y_n^m(\lambda,\mu) = -\frac{n(n+1)}{a^2} Y_n^m(\lambda,\mu). \tag{30}$$

While the gradient operator is similar to that of the torus in the zonal direction,

$$\frac{\partial}{\partial\lambda} Y_n^m(\lambda,\mu) = imY_n^m, \tag{31}$$

the meridional derivative of $Y_n^m(\lambda,\mu)$ is a recursion relation

$$\left(1-\mu^2\right)\frac{\partial}{\partial\mu} Y_n^m(\lambda,\mu) = -n\upsilon_{n+1,m} Y_{n+1}^m(\lambda,\mu) + (n+1)\upsilon_{n,m} Y_{n-1}^m(\lambda,\mu) \tag{32}$$

where $\upsilon_{n,m} = \left(\frac{n^2-m^2}{4n^2-1}\right)^{1/2}$. On the sphere, the Laplacian operator of a monochromatic source function is not equal to the square of the gradient operator. The simplification of the efficiency given in (28) from Shaw et al. [5] will not apply here. It will thus be necessary to find an alternative approach to solving for the analytic lower bound on $\mathcal{E}$ in spherical coordinates.

# 4 Upper Bounds and Péclet Number Scaling

The upper bound given in (27) from Shaw et al. [5] suggests that the efficiencies on the torus scale linearly in the Péclet number for large $Pe$. Thiffeault [6] also notes that for optimization problems on the torus, the optimal efficiencies scale quadratically for small $Pe$. Do these scalings in Péclet number hold for the sphere?

In order to determine the efficiencies of optimal flows, we must first solve the optimization problem given in (18). We can use the highly efficient, sub-optimal flows from Figure 2, namely the flows with $\psi \propto Y_3^2(\lambda,\mu)$ and $\psi \propto Y_2^2(\lambda,\mu)$ as initial guesses at $Pe = 10$ to obtain the two optimized flows shown in Figure 4.

Both flows in Figure 4 have characteristics similar to the efficient, but sub-optimal flows of Figure 2. The optimal flows tend to have stagnation points near the mean value of the source function and both have inter-hemispheric cells to transport the tracer from high concentrations at the equator to low concentrations near the poles. The efficiency of the optimized flow with $m = 2$ (Panel 4(a)) is slightly higher than that of the optimized flow

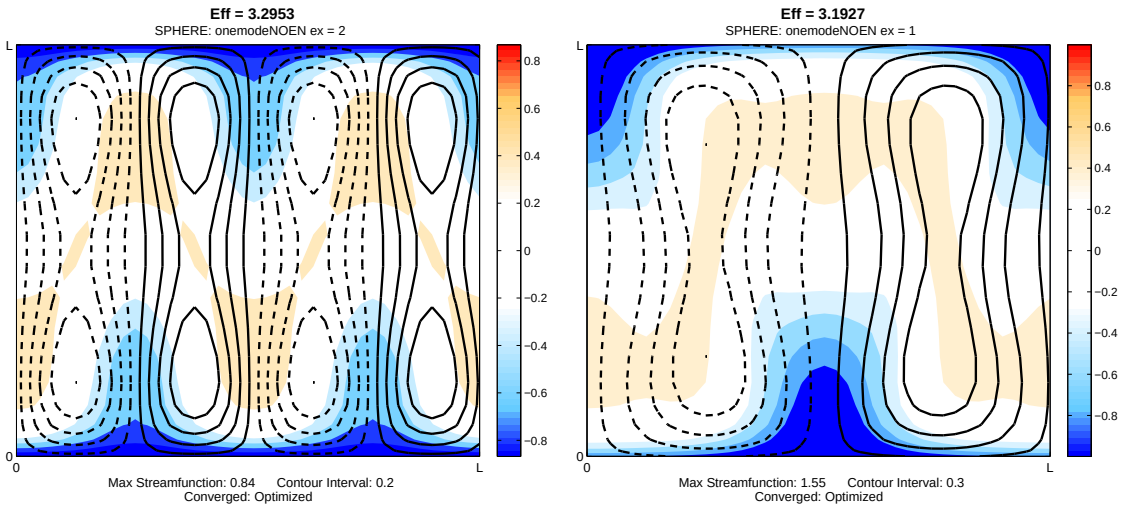


(a) Optimized Flow, $\mathcal{E} = 3.30$ (b) Optimized Flow, $\mathcal{E} = 3.19$

Figure 4: Two optimized flows with initial guesses guided by the efficient, sub-optimal flows $Y_2^2$ and $Y_3^2$ shown in Figure 2. Contours of the streamfunction are superimposed on filled, colored contours of the steady state tracer concentration.

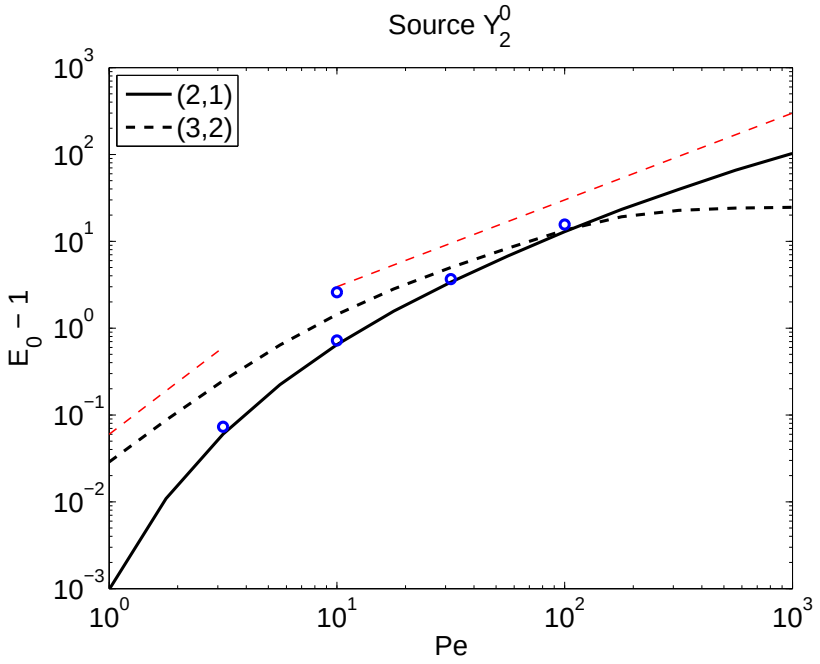


Figure 5: Efficiencies $\mathcal{E} - 1$ of optimized flows (blue circles) and sub-optimal flows (black lines) as a function changing Péclet number. The efficiencies of sub-optimal flows are those arising from streamfunctions proportional to $Y_3^2$ (dashed) and $Y_2^1$ (solid). Red dashed lines are the predicted scaling for the most efficient flows at low $Pe$ (quadratic scaling) and at high $Pe$ (linear scaling).

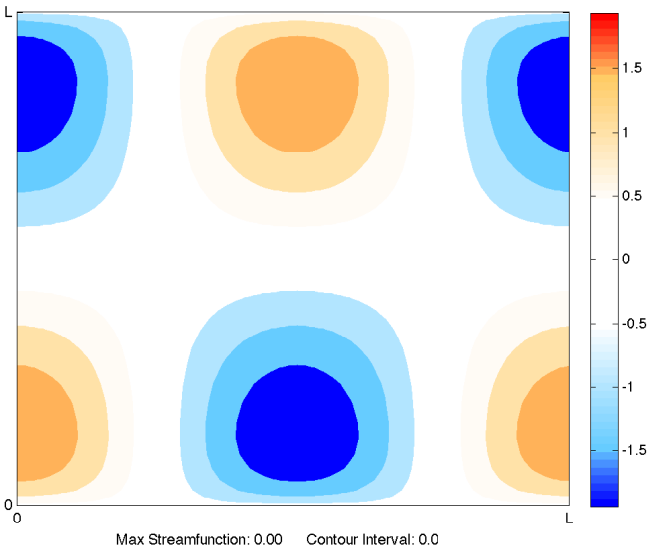


Figure 6: The cellular source on the sphere mapped in latitude-longitude coordinates.

with $m = 1$ (Panel 4(b)) at $\mathcal{E} = 3.30$ as compared to $\mathcal{E} = 3.19$. Expectedly, both flows have efficiencies greater than the most efficient sub-optimal flow in Figure 2.

While we were able to obtain these two optimal flows at $Pe = 10$, it was not without difficulty. As state in Section 2.3, the optimization algorithm for the sphere is an iterative process that will converge on local minima, if it converges at all. Unfortunately, due to time limitations, very few optimal solutions were found while for varying $Pe$. Those that we could identify are plotted in Figure 5 along with the efficiencies of sub-optimal flows. With the exception of one point at $Pe = 10$, most all optimized solutions lie very near that of the initial guess (the $Y_2^1$ mode).

In place of looking at the optimized flows, we examine the scaling of the efficiencies of the sub-optimal 'best guess' streamfunctions with monochormatic $Y_2^1$ or $Y_3^2$ modal structure instead of the true optimal solutions. From Figure 5, we see that the maximum efficiencies of the $Y_2^1$ and $Y_3^2$ modes appear to scale in agreement with the observations of Thiffeault [6] and of Shaw et al. [5] for the torus, namely that the mixing efficiencies scale as $Pe$ for small $Pe$ and transition to a $Pe^2$ scaling at high $Pe$.

The scaling of $\mathcal{E}$ with $Pe$ even holds if we move away from the geophysical source. If we consider a cellular source on the sphere (Figure 6) and its equivalent on the torus, we can compare the scaling of the efficiencies between the two geometries directly. The efficiencies of sub-optimal flows on the sphere (Panel 7(a)) and both optimal and sub-optimal flows on the torus (Panel 7(b)) are plotted against $Pe$ in Figure 7.

There are two primary observations to note in Figure 7: the close proximity of optimized flows on the torus to the sub-optimal cellular flows and the agreement with $Pe$ scaling arguments. For optimized flows on the torus, as with the optimized flows on the sphere in Figure 5, the optimal solutions lie very close to the 'best guess' sub-optimal flows. This suggests that the optimized efficiencies on the sphere for the cellular source should be

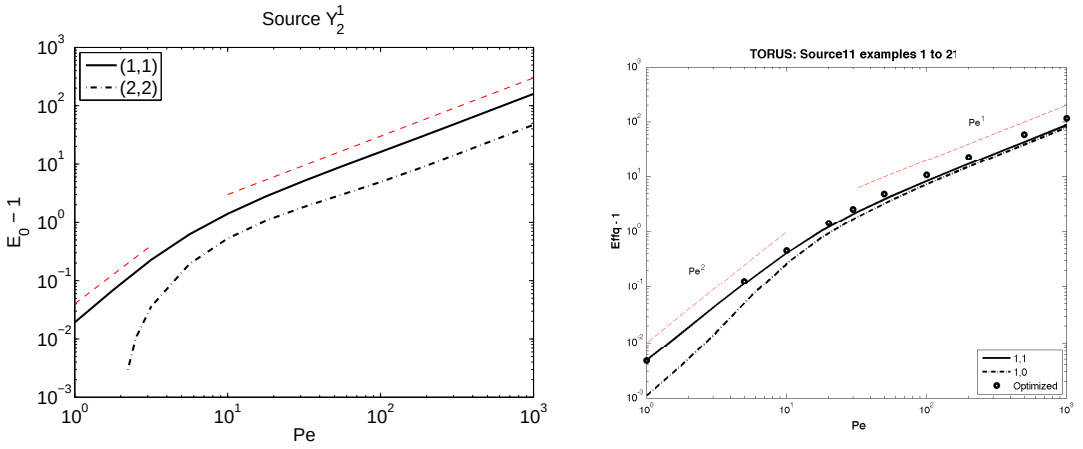


(a) Sphere (b) Torus

Figure 7: Scaling of efficiencies $\mathcal{E} - 1$ with respect to changing $Pe$ for the cellular source function (shown in Figure 6 for the sphere) on the sphere (Panel 7(a)) and for the equivalent flow on the torus (Panel 7(b)). Efficiencies of sub-optimal flows of $Y_1^1$ (solid) and $Y_2^2$ (dashed) over the surface of the sphere are shown in Panel 7(a). Similarly, sub-optimal flows on the torus are shown for $k_x = 1$, $k_y = 1$ (solid) and $k_x = 1$, $k_y = 0$ (dashed) in Panel 7(b). Optimized flows for the torus are shown in circles. Quadratic and linear $Pe$ slopes are red-dashed.

relatively close to the sub-optimal flows shown in Figure 7, however this still needs to be shown in future work.

The close agreement to the $Pe$ scaling between the torus and the sphere suggests that, unlike the lower bound on $\mathcal{E}$, one property of maximally efficient flows from the torus does carry over to the sphere. Why, then, does the efficiency scale linearly in $Pe$ at high $Pe$ and as $Pe^2$ at small $Pe$? Why is this result independent of geometry?

At high $Pe$, we can approximate the effect of stirring by and eddy diffusivity, $\kappa_{eff}$, that is significantly larger than the molecular diffusivity, $\kappa$. For an advection-dominated regime, an effective diffusivity can be generated by $\kappa_{eff} \sim UL$, where $U$ is the characteristic length of the advective velocity and $L$ is a characteristic mixing length [4, 5]. For the cellular flows we've considered here, where the most efficient flows tend to be those of the largest scale permissible, the characteristic length scale is that of the domain for the torus or that of radius for the sphere.

The stirred steady state advection-diffusion equation (1) is then parameterized by

$$\kappa_{eff} \Delta\theta \approx s \tag{33}$$

while the unstirred, diffusive steady state problem is unchanged

$$\kappa \Delta\theta_0 = s \tag{34}$$

so that the solutions to the steady state stirred and unstirred systems are

$$\theta \approx \frac{1}{\kappa_{eff}} \Delta^{-1} s \qquad\qquad \theta_0 = \frac{1}{\kappa} \Delta^{-1} s. \tag{35}$$

The efficiency $\mathcal{E}$ is then approximated by

$$\mathcal{E} = \sqrt{\frac{\langle|\theta_0|^2\rangle}{\langle|\theta|^2\rangle}} \approx \sqrt{\frac{\kappa^{-2}\langle|\Delta^{-1}s|^2\rangle}{\kappa_{eff}^{-2}\langle|\Delta^{-1}s|^2\rangle}} \tag{36}$$

which scales as

$$\mathcal{E} \sim \frac{\kappa_{eff}}{\kappa} \sim \frac{UL}{\kappa} = Pe \tag{37}$$

where we have used $\kappa_{eff} \sim UL$. From (37), the mixing efficiency $\mathcal{E}$ should scale linearly with $Pe$ so long as $Pe$ is sufficiently large such that the mixing is advection-dominated and the advection-diffusion equation can be approximated by an eddy diffusivity.

The diffusion-dominated small $Pe$ regime, on the other hand, appears to scale quadratically in $Pe$ for the cases we have considered here. Consider the advection-diffusion operator $\mathcal{L}$ given in (9) in the limit of small $Pe$. By definition the Péclet number is the scale of the advection term relative to the diffusive term in (1) and could be considered a small parameter in the steady-state, nondimensional advection-diffusion equation

$$\left(Pe\hat{\boldsymbol{u}}\cdot\hat{\boldsymbol{\nabla}} - \hat{\Delta}\right)\hat{\theta} = \hat{s} \tag{38}$$

where hatted variables are nondimensional. We have assumed here that, to a first approximation, the size of the source function scales as $\Delta\theta$ in the limit of small $Pe$.

The inverse of the nondimensional operator $\hat{\mathcal{L}}^{-1} = \left(Pe\hat{\boldsymbol{u}}\cdot\hat{\boldsymbol{\nabla}} - \hat{\Delta}\right)^{-1}$ can then be approximated by expanding about $Pe \ll 1$. Let $A = \hat{\boldsymbol{u}}\cdot\hat{\boldsymbol{\nabla}}$ be the advection operator and let $D = -\hat{\Delta}$ be the diffusion operator. Additionally, let $\epsilon = Pe$ be the small parameter. The nondimensional advection-diffusion operator (dropping the hats) is then

$$\mathcal{L} = D + \epsilon A. \tag{39}$$

The inverse of (39) can then be expanded out to $O(\epsilon)$

$$\mathcal{L}^{-1} = D^{-1} - \epsilon D^{-1}AD^{-1} + O(\epsilon^2) \tag{40}$$

such that $\langle|\theta|^2\rangle = \langle|\mathcal{L}^{-1}s|^2\rangle$ is

$$\begin{aligned}\langle|\theta|^2\rangle &= \frac{1}{V}\int\left(\mathcal{L}^{-1}s\right)^2 dV \\ &= \frac{1}{V}\int\left(D^{-1}s - \epsilon D^{-1}AD^{-1}s + O(\epsilon^2)\right)^2 dV\end{aligned} \tag{41}$$

Expanding the square of (41) yields

$$\langle|\theta|^2\rangle = \frac{1}{V}\int\left(D^{-1}s\right)^2 - 2\epsilon\left(D^{-1}s\right)\left(D^{-1}AD^{-1}s\right)dV + O(\epsilon^2) \tag{42}$$

The advection operator can be written in terms of, $A\xi = [\psi,\xi]$, where

$$[\psi,\xi] = \frac{\partial\psi}{\partial x}\frac{\partial\xi}{\partial y} - \frac{\partial\xi}{\partial x}\frac{\partial\psi}{\partial y} = v\frac{\partial\xi}{\partial y} + u\frac{\partial\xi}{\partial x} \tag{43}$$

on the torus, noting that the non-divergent advective velocities are defined using a streamfunction $\psi$ by $u = -\frac{\partial \psi}{\partial y}$ and $v = \frac{\partial \psi}{\partial x}$. On the sphere,

$$[\psi, \xi] = \left(\frac{1}{a\cos\phi}\frac{\partial \psi}{\partial \lambda}\right)\left(\frac{1}{a}\frac{\partial \xi}{\partial \phi}\right) - \left(\frac{1}{a\cos\phi}\frac{\partial \xi}{\partial \lambda}\right)\left(\frac{1}{a}\frac{\partial \psi}{\partial \phi}\right) \tag{44}$$

for the non-divergent velocities given in (21).

Replacing the advection operator in (42) with $[\psi, \xi]$ yields

$$\langle|\theta|^2\rangle = \frac{1}{V}\int \left(D^{-1}s\right)^2 - 2\epsilon\left(D^{-1}s\right)\left(D^{-1}[\psi, D^{-1}s]\right) dV + O(\epsilon^2) \tag{45}$$

such that the variation in $\langle|\theta|^2\rangle$ given a change in the streamfunction $\delta\psi$ is

$$\delta\langle|\theta|^2\rangle = -\frac{2\epsilon}{V}\int \left(D^{-1}s\right) D^{-1}\left[\delta\psi, D^{-1}s\right] dV + O(\epsilon^2) \tag{46}$$

$$= -\frac{2\epsilon}{V}\int \delta\psi\left[D^{-1}s, D^{-2}s\right] dV + O(\epsilon^2). \tag{47}$$

To $O(\epsilon^2)$, the variation of $\langle|\theta|^2\rangle$ is then

$$\frac{\delta\langle|\theta|^2\rangle}{\delta\psi} = -2\epsilon\langle\left[D^{-1}s, D^{-2}s\right]\rangle + O(\epsilon^2). \tag{48}$$

For any source that satisfies $\left[D^{-1}s, D^{-2}s\right] = 0$, such as monochromatic sources, the variation of $\langle|\theta|^2\rangle$ with respect to a change in the streamfunction $\delta\psi$ will be zero at $O(\epsilon)$. As both the geophysical and the cellular sources considered here are monochromatic, we can expect $\langle|\theta|^2\rangle$ to vary as $\epsilon^2 = Pe^2$, hence the quadratic scaling in the Péclet number at small $Pe$. If we were to instead look flows which optimized $\mathcal{E}$ on the sphere with a source function satisfying $\left[D^{-1}s, D^{-2}s\right] \neq 0$, we might expect linear scaling at small $Pe$. Experiments so far, however, have been inconclusive. Finding sources where efficiencies scale linearly in $Pe$ is left for future work.

# 5 Sweeping Flow

It is interesting to note that the $Y_3^2$ flow appears to saturate in efficiency around $Pe = 10^2$ in Figure 5 for the geophysical source. This saturation leads to a crossing of the efficiencies of sub-optimal flows. Although streamfunctions with a modal structure of $Y_3^2$ are more efficient mixers than those of $Y_2^1$ at small $Pe$, $Y_2^1$ is more efficient than the $Y_3^2$ mode at high $Pe$.

The saturation of $\mathcal{E}$ at high $Pe$ for the $Y_3^2$ streamfunction can be understood by looking at the steady state snapshots of $\theta$ and $\psi$ in Figure 8. At $Pe = 10^3$, the tracer field becomes trapped near the stagnation points of $\boldsymbol{u}$. For the saturated streamfunction in Panel 8(b), the flow velocity is largely parallel to contours of constant $\theta$ in steady state such that the velocity field is no longer stirring the tracer field as, for these flows, $\boldsymbol{u}\cdot\nabla\theta \approx 0$. As the advective term of (7) is small, increasing the Péclet number further by either decreasing the diffusivity or increasing the strength of the velocity field $\boldsymbol{u}$ will do little to change the mixing efficiency, hence $\mathcal{E}$ will not change greatly with increasing $Pe$ as observed in Figure 5.

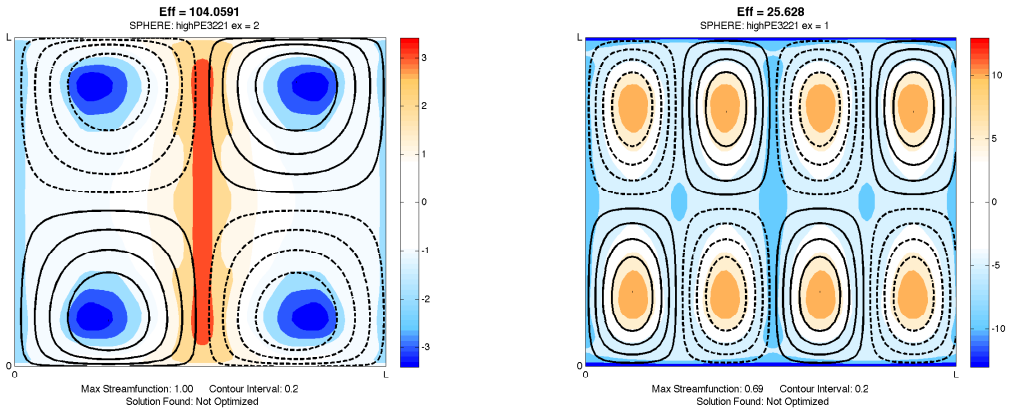


(a) High $Pe$, $\mathcal{E} = 104.06$, $Y_2^1$

(b) High $Pe$, $\mathcal{E} = 25.63$, $Y_3^2$

Figure 8: Flows given with a streamfunction structure of $Y_2^1$ in Panel 8(a) and $Y_3^2$ in Panel 8(b) at $Pe = 10^3$ in the region of efficiency saturation. Streamlines (black) are superimposed on colored contours of the stirred, steady-state $\theta$.

We are interested in finding the velocity field that most efficiently mixes the a tracer over the surface of the sphere for a given source function, however we have only considered time independent velocity fields that contain stagnation points in $\boldsymbol{u}$. The presence of these stagnation points limits the mixing efficiency of these steady flows at high $Pe$. We may be able to achieve higher $\mathcal{E}$ if we allow the flow to vary in time such as to effectively remove these stagnation points on average.

One example of such an efficient, time-varying flow for the torus is found in Shaw et al. [5]. Shaw et al. [5] are able to saturate the upper bound of $\mathcal{E}$ given in (27) using a 'sweeping' flow. This flow is characterized by a constant velocity, $U$, that alternates between a purely zonal flow and a purely meridional flow over the torus over long timescales. Does such a sweeping flow exist for the sphere?

A sweeping flow as described in Shaw et al. [5] for the torus cannot be defined on the sphere in the same manner as it is on the torus due to the presence of the poles. The velocity field $\boldsymbol{u}$ must be zero at the poles because of artificial discontinues in the gradient operator in spherical coordinates. If we were to consider a velocity field that was purely zonal at one instant in time it would be require to have the amplitude of $\boldsymbol{u} = u(\phi)\hat{\lambda}$ to go to zero as $\phi \to \pm 90°$. A rotation of this flow by 90° on the sphere would not produce the same purely meridional flow as in the sweeping flow on the torus. Instead, it would produce a flow with strong meridional velocities over the poles and with two stagnation points at the equator. With a fixed coordinate system this rotated flow violates the condition that $|\boldsymbol{u}| = 0$ at the poles.

A sweeping flow on the sphere would then require more than just a rotation of the velocity field. One method to obtain a sweeping flow on the sphere is described by Finn [2]. Finn [2] considers a sweeping flow produced by a rotation of both the velocity field and the source function or, equivalently, a rotation of the coordinate system.

Perhaps the simplest sweeping flow over the sphere would have an initial velocity field

$$\boldsymbol{u} = \sqrt{\frac{3}{2}} U \cos(\phi) \hat{\lambda} \tag{49}$$

mixing a tracer supplied by the source function given by

$$s(\lambda, \mu) = S P_1(\mu) \left( \exp\left(-i\lambda\right) + \exp\left(i\lambda\right) \right) = S \left( Y_1^1(\lambda, \mu) + Y_1^{-1}(\lambda, \mu) \right). \tag{50}$$

This source function is not identical to the rotate geophysical source. It instead describes a sphere heated in the western hemisphere and cooled in the eastern hemisphere. We choose this particular source instead of the rotated geophysical source in Finn [2] as simplifies the advective term significantly upon rotation of the velocity field.

We allow the velocity field given in (49) to mix the source from (50) to steady state before rotating the velocity field by 90°. Upon rotation, the velocity field will lie parallel to lines of constant $\phi$ as supplied by the source function $s(\lambda, \mu)$ from (50) such that $\boldsymbol{u} \cdot \nabla \theta = 0$. As the velocity field does not advect the tracer away from the source, all stirring enhanced mixing occurs in the first half of the sweeping flow when $\boldsymbol{u}$ is given by (49).

The mixing efficiency of the sweeping flow given by (49) over the sphere can be calculated by first finding the steady state tracer concentration satisfying the steady-state advective diffusive equation of (7). Using the gradient and Laplacian formulations given in (31) and (30), the tracer concentration in steady state satisfies

$$\begin{aligned} \sqrt{\frac{3}{2}} \frac{U}{a} \left( \sum_{n=0}^{\infty} \sum_{m=-n}^{n} im \tilde{\theta}_n^m Y_n^m(\lambda, \mu) \right) + \kappa \sum_{n=0}^{\infty} \sum_{m=-n}^{n} \frac{n(n+1)}{a^2} \tilde{\theta}_n^m Y_n^m(\lambda, \mu) \\ = S \left( Y_1^1(\lambda, \mu) + Y_1^{-1}(\lambda, \mu) \right) \end{aligned} \tag{51}$$

such that the we can solve for the $\tilde{\theta}_n^m$ by matching coefficients,

$$\begin{aligned} \tilde{\theta}_1^{-1} &= S \left( -i \sqrt{\frac{3}{2}} \frac{U}{a} + \kappa \frac{2}{a^2} \right)^{-1} \\ \tilde{\theta}_1^{1} &= S \left( +i \sqrt{\frac{3}{2}} \frac{U}{a} + \kappa \frac{2}{a^2} \right)^{-1}. \end{aligned} \tag{52}$$

By Parsevals' theorem, the variance of $\theta$ is then

$$\langle |\theta|^2 \rangle = 2\pi \sum_{n=0}^{\infty} \sum_{m=-n}^{n} \left| \tilde{\theta}_n^m \right|^2 \tag{53}$$

which, given the coefficients from (52), allows us to find the steady state tracer variance of the stirred problem

$$\langle |\theta|^2 \rangle = 4\pi S^2 \left( 4 \frac{\kappa^2}{a^4} + \frac{3}{2} \frac{U^2}{a^2} \right)^{-1}. \tag{54}$$

By taking $U = 0$ in (54), we can similarly find the steady state tracer variance of the unstirred problem

$$\langle |\theta_0|^2 \rangle = 4\pi S^2 \left( 4\frac{\kappa^2}{a^4} \right)^{-1} \tag{55}$$

we can calculate the efficiency of the sweeping flow as

$$\mathcal{E}^2 = \frac{\langle |\theta_0|^2 \rangle}{\langle |\theta|^2 \rangle} = \frac{a^4}{4\kappa^2} \left( 4\frac{\kappa^2}{a^4} + \frac{3}{2}\frac{U^2}{a^2} \right) = 1 + \frac{3}{8}Pe^2 \tag{56}$$

where $Pe = \frac{Ua}{\kappa}$.

If we were to compare the mixing efficiency of the sweeping flow over the sphere to the upper bound for the mixing efficiency of a monochromatic source similar to that of (50) on the torus in (27), we would expect that the most efficient sweeping flow over the torus would have a mixing efficiency of

$$\mathcal{E}^2_{torus} = 1 + \frac{1}{2}Pe^2 \tag{57}$$

where the source function on the $d = 2$ torus is described by

$$s(x, y) = S_{torus}(e^{ix} + e^{-ix}) \tag{58}$$

in a domain of length $L = 1$ with a total wavenumber of $k_s^2 = 1$.

In comparing (56) to (57), we note that the mixing efficiency of the sweeping flow on the sphere is very close to that of the torus. The effiency $\mathcal{E}^2$ of the sweeping flow on the sphere scales as $\frac{3}{8}Pe^2$ as compared to a scaling of $\frac{1}{2}Pe^2$ on the torus. For the same Péclet number, the sweeping flow over the torus will be slightly more efficient than the corresponding sweeping flow on the sphere.

Additionally, the sweeping flow over the sphere has an efficiency $\mathcal{E} = \sqrt{1 + \frac{3}{8}Pe^2}$ which scales as

$$\mathcal{E} \approx \begin{cases} \sqrt{\frac{3}{8}}Pe & \text{for } Pe \gg 1 \\ 1 + \frac{3}{16}Pe^2 & \text{for } Pe \ll 1 \end{cases} \tag{59}$$

such that $\mathcal{E}$ scales linearly in $Pe$ at high $Pe$ and quadratically in $Pe$ at low $Pe$ in agreement with the arguments for highly efficient flows found in Section 4.

While Shaw et al. [5] found that the sweeping flow on the torus is the most efficient flow for a monochromatic source function, we are not guaranteed that the sweeping flow described by (49) is the most efficient flow for the the sphere. One particular issue with any flow on the sphere arises due to the location of stagnation points in the flow.

As we must have $|\boldsymbol{u}| = 0$ at the poles for any rotated coordinate system we choose, we will always have stagnation points in the velocity field over the poles. It would then always be possible to achieve the trapping behavior described for inefficient flows in Section 3 if these polar stagnation points are located away from the mean value of the source function. (One could consider regions where the source is equal to its mean as already well-mixed, thus stirring by $\boldsymbol{u}$ could do little to reduce the variance in these regions.) This is one reason

why we chose the source given in (50) rather than the rotated geophysical source. The rotate geophysical source from Finn [2], given by

$$s(\lambda,\mu) = -\frac{\sqrt{3}}{2} SP_2^2(\mu)\left(\exp\left(-2i\lambda\right) + \exp\left(2i\lambda\right)\right) + \frac{1}{\sqrt{2}} SP_2^0\left(\mu\right), \tag{60}$$

would have a maxima over the poles. These regions could never be mixed for a fixed spherical coordinate system, leading to a saturation of $\mathcal{E}$ with increasing $Pe$ similar to the suboptimal flows stirred by a streamfunction proportional to $Y_3^2$ in Figure 5 and in Panel 8(b).

Finn [2] suggests a more efficient sweeping flow could be achieved by a careful rotation of the coordinate system at each time interval. If the poles of the spherical coordinate system are always located in regions where the source function achieves its mean value one could bypass the trapping issue on the sphere and possibly find the most efficient, time-dependent flows on the sphere.

# 6 Discussion and Future Directions

In this work we sought answers to the two following questions: 1) what flows most efficiently mix a tracer field on the surface of the sphere that is supplied by a spatially-varying source function? and 2) how do the properties of these flows compare to similar velocity fields on the torus? We were able to find flows that maximized the mixing efficiency given in (5) using a numerical optimization scheme. This optimization scheme, however, only optimizes the velocity field according to one measure of the mixing efficiency. In determining the flows that maximize other possible measures of mixing efficiency, such as the multi-scale mixing efficiencies described in Shaw et al. [5] given by

$$\mathcal{E}_p^2 = \frac{\langle|\nabla^p\theta_0|^2\rangle}{\langle|\nabla^p\theta|^2\rangle} \tag{61}$$

where $p = -1, 0, 1$, we could emphasize the homogenization of variance of $\theta$ on smaller ($p = 1$) and larger ($p = -1$) spatial scales.

In changing geometries we find that many of the properties of optimized flows over the torus do not translate directly to that of the sphere. The hard lower bound of $1 \leq \mathcal{E}$ of Shaw et al. [5], for example, is violated for the geophysical source on the sphere due to the inescapable presence of stagnation points in $\boldsymbol{u}$ and the trapping of the tracer concentration at its source.

The issue of stagnation points in the stirring field on the sphere also has consequences for saturating an upper bound, should such an upper bound be discovered in the future. To remove these stagnation points we must consider time-dependent velocity fields similar to the sweeping flow described by Shaw et al. [5] modified by the solid body rotation method introduced by Finn [2]. It may be possible to determine the most efficient time-dependent flow for a given source function on the sphere by using the method of steepest decent described in Lin et al. [3].

One similarity between efficiencies of optimal (or sub-optimal, in the case of the sphere) flows for the two geometries is that of the scaling of $\mathcal{E}$ with changing $Pe$. For both the geophysical and the cellular source functions, the efficiency $\mathcal{E}$ scales linearly with $Pe$ at high

$Pe$ and quadratically with $Pe$ at small $Pe$. For diffusion-dominated flows at small Péclet number we expanded the advection-diffusion integral operator, $\mathcal{L}^{-1}$ around the diffusive term and determined that the $\mathcal{E} \sim Pe^2$ scaling in this regime was a consequence of our choice of monochromatic sources. It is an open question as to whether we can obtain linear Péclet number scaling for non-monochromatic sources, such as sources with off-equatorial heating.

As we are motivated here by the geophysical question of the redistribution of heat over the surface of the sphere, the optimization of $\mathcal{E}$ subject to more complex source functions are of significant interest. Some source functions in particular are those with off-equatorial heating, as mentioned, to simulate seasonal changes in solar insolation. Additional source functions we could consider include those with longitudinally localized heating to simulate land-sea surface temperature contrasts.

Throughout this work we have considered a velocity field that is independent of temperature, however in a geophysical context these two fields are not wholly independent. It may be of further interest to modify the code to allow for coupling between the velocity field and the tracer field.

The energy constraint here follows from previous work on the torus. However, this is not the only dynamical constraint we may wish to explore on the sphere. If we were to include some form of rotation to our model of optimized flows over the sphere, we could additionally consider an angular momentum constraint in the form of

$$M = \Omega a^2 \cos^2 \phi + ua \cos \phi \tag{62}$$

where $M$ is the angular momentum, $\Omega$ is the rotation rate, $a$ is the radius of the sphere, and $u$ is the zonal component of the non-divergent velocity field $\boldsymbol{u}$.

On the Earth, the redistribution of heat on the sphere from large-scale atmospheric stirring is not primarily achieved by the barotropic circulations we have considered here, but instead by the near-zonally symmetric circulations of the Hadley and Ferrel cells in height $z$ and latitude $\phi$ coordinates. A question of significant geophysical interest would then be what zonally symmetric circulation pattern in $z$-$\phi$ coordinates most efficiently mixes temperature on the sphere? Furthermore, can such a flow be obtained using a numerical optimization scheme such as the one used here?

# 7 Acknowledgements

I would foremost like to thank Tiffany Shaw and Jean-Luc Thiffeault for their guidance and advice throughout the summer, particularly in the final days of the program when everything came together. The GFD program wouldn't be the same without softball; I would like to thank George Veronis and Charlie Doering for their coaching and endless enthusiasm through the summer's practices, games, and injuries. Last, but certainly not least, I'd like to thank my fellow fellows–Anubhab, David, Emma, Renske, Georgy, Kiori, Michael, Sam, and Woosok–for all the late nights in Walsh Cottage, fantastic dinners, trips to the beach, and more.

## References


[1] J. B. Drake, P. Worley, and E. D'Azevendo, *Algorithm 888: Spherical harmonic transform algorithms*, ACM Trans. Math. Softw., 35 (2008), pp. 23:1–23.

[2] M. D. Finn, *Mixing on the sphere.* notes, 2010.

[3] Z. Lin, J.-L. Thiffeault, and C. R. Doering, *Optimal stirring strategies for passive scalar mixing.* Under consideration for publication in J. Fluid Mech., 2010.

[4] J. M. Ottino, *Mixing, chaotic advection, and turbulence.*, Annu. Rev. Fluid Mech., 22 (1990), pp. 207–253.

[5] T. A. Shaw, J.-L. Thiffeault, and C. R. Doering, *Stirring up trouble: Multi-scale mixing measures for steady scalar sources*, Physica D, 231 (2007), pp. 143–164.

[6] J.-L. Thiffeault, *Quantifying fluid mixing using norms.* in preparation, 2010.

[7] J.-L. Thiffeault, C. R. Doering, and J. D. Gibbon, *A bound on mixing efficiency for the advection–diffusion equation*, J. Fluid Mech., 521 (2004), pp. 105–114.

[8] J.-L. Thiffeault and G. A. Pavliotis, *Optimizing the source distribution in fluid mixing*, Physica D, 237 (2008), pp. 918–929.